Desalination and Water Treatment
www.deswater.com
doi: 10.1080/19443994.2014.927332

55 (2015) 1620–1628
July

Taylor & Francis
Taylor & Francis Group

Adsorption of metronidazole in aqueous solution by Fe-modified sepiolite

Hua Ding[a,*], Guangrong Bian[b]

[a]*School of Earth Science and Resources, Chang'an University, 126 Yanta Road, Xi'an 710054, Shaanxi Province, P.R. China, email: 1691423259@qq.com*
[b]*Department of Aviation Ammunition, Air Force Service College, 227 Zhongshan Road, Xuzhou 221003, Jiangsu Province, P.R. China, email: 44973901@qq.com*

Received 30 October 2013; Accepted 14 May 2014

ABSTRACT

Metronidazole (MET), a widely used antibiotic, has attracted more attention for its highly solubility, non-biodegradability, and suspected carcinogen. The original sepiolite and its modified counterparts were prepared by different methods and characterized by SEM, XRD, and BET. The specific surface area and pore volume of the Fe-modified sepiolite were 217.68 m^2/g and 3.8743 cm^3/g, respectively, with 19 and 215% increment compared with the original sepiolite. The samples were used to remove MET from aqueous solutions. The effects of pH, contact time, initial MET concentration, and temperature on the adsorption process were investigated. It was found that the Fe-modified sepiolite had higher adsorption capability (36.5%) for MET than that of others. The MET adsorption on the Fe-modified sepiolite was fast and the process conformed to the pseudo-second-order kinetic model, and the adsorption equilibrium data fitted well with the Freundlich isotherms.

Keywords: Adsorption; Metronidazole; Fe-modified sepiolite; Kinetics; Thermodynamics

1. Introduction

Pharmaceuticals and personal care products (PPCPs) are continuously being introduced into the aquatic environment [1–4], due to their widespread use in humans and animals [5]. Since early 1980s, several studies investigated the presence of pharmaceuticals and related metabolites in aquatic environment [1,6]. Recently, the PPCPs were considered as an emerging environmental problem due to their continuous input and persistence to the aquatic ecosystem even at low concentrations [7]. Some technologies have been evaluated to decrease PPCPs discharge into water bodies, e.g. photodegradation [8,9], biodegradation [10–12], activated carbon, and membrane filtration adsorption [13,14]. However, the methods mentioned above are too costly to use on a large scale [15].

Clays like sepiolite [16–24], attapulgite [25], montmorillonite [26,27], kaolin [26,27], rectorite [28,29], bentonite [30], and mica [31], have attracted attention due to their specific properties and structures, abundance, and low cost. Among clays, sepiolite is more attractive as it has relatively high specific surface area and adsorption capacity. Özcan et al. [16] and Tabak et al. [17] studied the adsorption properties of sepiolite for the removal of dyes from aqueous solutions. Rytwo et al. [18] investigated the adsorption capacity of sepiolite for two organic cations (methylene blue and crystal violet) and two neutral

*Corresponding author.

1944-3994/1944-3986 © 2014 Balaban Desalination Publications. All rights reserved.

organic molecules (Triton-X 100 and crown ether 15-crown-5). They found that the free negative sorption sites and neutral sorption sites on the surface of sepiolite contributed to the adsorption of organic molecules. Alkan et al. [20] treated sepiolite with organosilanes and discussed the interactions between sepiolite surface and organosilane molecules, and then they analyzed the electrokinetic properties of the modified sepiolite using FTIR and zeta measurements. Park [21] applied organic surfactant-modified clays to water purification. Akçay [23] prepared Fe-pillared sepiolite from Anatolia and compared the adsorption of pyridine on original sepiolite and Fe-pillared sepiolite.

Drug metronidazole (MET) is an antibiotic which is widely used for the treatment of infections caused by anaerobic bacteria and various protozoans [32–35]. The structure of MET is shown in Fig. 1. The MET has attracted more attention because it is highly soluble, non-biodegradable, and a suspected carcinogen [5,12]. Johnson et al. [5] degraded MET in aqueous solution by UV/H_2O_2 process in single- and multi-lamp tubular photoreactors. The maximum removal of MET were 13 and 41% for the single-lamp and multi-lamp photoreactors, respectively. Dantas et al. [33] studied direct photolysis of MET in aqueous solution promoted by ultra violet radiation (UV). Lam et al. [35] studied the adsorption of MET on clinoptilolite by means of computational simulations.

In the present study, several kinds of modified sepiolites were prepared and used for the adsorption of MET in aqueous solutions. Then, adsorption experiments were carried out to remove MET from aqueous solutions using Fe-modified sepiolite (Fe–S). The effects of pH, contact time, initial MET concentration, and temperature on the adsorption of MET were investigated. The kinetics and thermodynamics of the adsorption were studied as well.

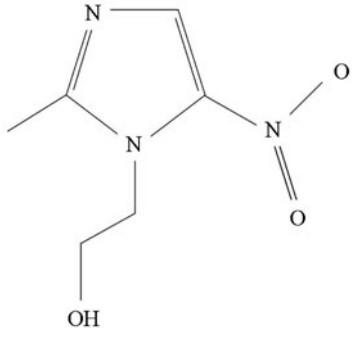

Fig. 1. Chemical structure of MET.

2. Materials and methods

2.1. Materials

The sepiolite used in this study was manufactured by Liuyang sepiolite Co., Ltd (Liuyang, P.R. China). Ferric nitrate ($Fe(NO_3)_3{\cdot}9H_2O$), sodium carbonate (Na_2CO_3), sodium hydroxide (NaOH), and hydrochloric acid (HCl) were manufactured by Sinopharm Chemical Reagent Co., Ltd (SCRC, China), all the reagents were analytical reagent grade and used without further purification. The MET was commercially available grade. Deionized water was used throughout the experiment.

2.2. Preparation

The modified sepiolite samples include Na-modified sepiolite (Na–S), Fe-modified sepiolite (Fe–S), and Fe–Na-modified sepiolite (Fe–Na–S); Fe–S calcined at 673 K (Fe–S-673), and Fe–Na–S calcined at 673 K (Fe–Na–S-673). The Na–S composites were prepared by the interaction of clay and NaCl [28]. The Fe–S composites were prepared by the following steps: (1) The pillaring solution was prepared by adding a 0.2 mol/L Na_2CO_3 solution dropwise into a 0.4 mol/L $Fe(NO_3)_3$ solution under stirring at 298 K, up to a Na/Fe molar ratio of 1. (2) The pillaring solution was aged for 24 h at 298 K, and then was added dropwise into a 2 wt% sepiolite aqueous suspension under stirring at 333 K to obtain a ratio of 10 mmol of Fe/g of sepiolite. (3) After the resulting suspension was aged for 8 h at 333 K, the precipitate was separated by centrifuging and washed with deionized water. Then the Fe–S composites were obtained after being dried in air at 343 K for 5 h. The Fe–Na–S composites were prepared using the same method as the Fe–S composites except for the replacement of sepiolite by Na–S composites. The Fe–S-673 composites and Fe–Na–S-673 composites were obtained after the Fe–S composites and Fe–Na–S composites were calcined at 673 K for 3 h, respectively.

2.3. Adsorption

The composites (0.2 g) were mixed in 100 mL of MET aqueous solutions with different concentrations (10–30 mg/L). The pH values of initial solutions were adjusted with diluted HCl (6 mol/L) or NaOH (4 mol/L) solution using a pH meter (Mettler Toledo Group, Delta 320). The mixtures were shaken (200 rpm) in a thermostatic shaker bath (THZ-82 mechanical shaker, Changzhou Guohua Instruments, China) at desired temperature and contact time, and then the suspensions were centrifuged to remove the

composites. The absorbance of the MET aqueous solution was analyzed using a UV–vis spectrophotometer (UV-2102, UNICO, China) at its maximum absorption wavelength of 320 nm. The MET concentrations were calculated by the adsorption calibration curve of MET aqueous solution. The adsorption capacity of the composites was calculated using Eq. (1),

$$q_e = (C_0 - C_e)V/m \quad (1)$$

where q_e is the adsorption capacity of MET by the composites (mg/g), C_0 is the initial concentration of the MET (mg/L), C_e is the equilibrium MET concentration (mg/L), m is the mass of the composites (g), and V is the volume of the MET solution (L).

2.4. Characterization

The morphologies of the original sepiolite and the Fe–S composites were examined using scanning electron microscope (SEM, JSM-5610LV). The structure and crystallinity of the original sepiolite and the Fe–S composites were characterized by an X-ray diffractometer (XRD, Rigaku D/MAX-RB) with Cu Kα radiation under the operation conditions of 40 kV and 50 mA. Nitrogen sorption isotherms were obtained by a Tristar 3000 instrument (Micromeritics, USA); the surface area and pore size were measured by BET (Brunauer–Emmett–Teller) method; the samples were degassed at 100 ℃ overnight prior to measurement.

3. Results and discussion

3.1. Effect of modification methods

The removal test results are shown in Fig. 2. The results showed that the adsorption capacity of Fe–S composites (36.5%) is higher than that of the original sepiolite (8.3%) and the sepiolite modified by other methods. The adsorption capacity of the prepared composites is in the order of Fe–S > Fe–Na–S > original sepiolite > Fe–S-673 > Na–S > Fe–Na–S-673. Thus, the Fe–S composites were chosen for further study.

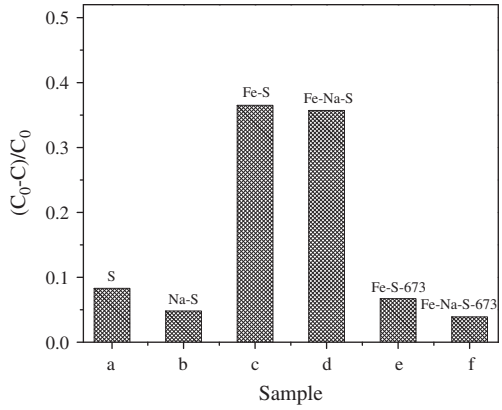

Fig. 2. Uptake of the MET in the aqueous solutions over different samples: (a) S; (b) Na–S; (c) Fe–S; (d) Fe–Na–S; (e) Fe–S-673; (f) Fe–Na–S-673. [MET] = 10 mg/L, amount of Fe–S 0.2 g, pH 7.0, at 303 K.

3.2. Characterization

The SEM images of the original sepiolite and Fe–S composites are shown in Fig. 3. The original sepiolite presents smooth and dense surface while the Fe–S composites refer to relatively rough surface and loose structure, indicating iron hydroxide might partly destroy the mineral congeries, and then the surface of the sepiolite was cracked. The XRD patterns of the original sepiolite, Fe–S, and Fe–S-673 composites are shown in Fig. 4. For the original sepiolite and the Fe–S composites, the basal X-ray reflection values of the (110) peak (d_{110}) were found to be 12.07 and 12.20 Å,

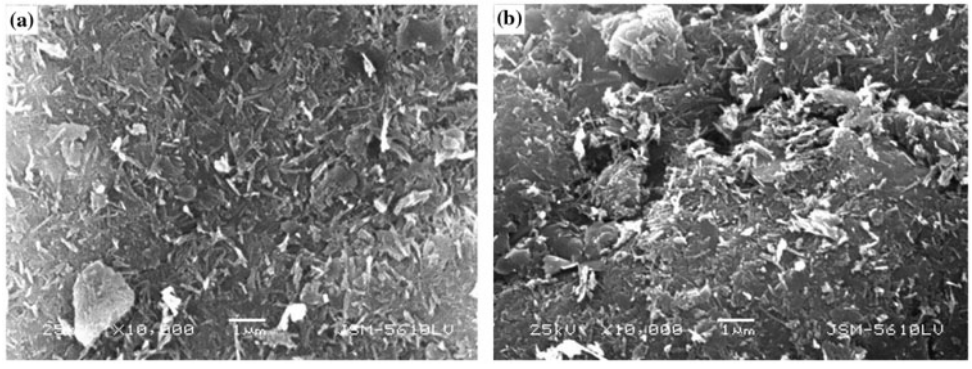

Fig. 3. SEM images of the as-prepared composites (a) S and (b) Fe–S.

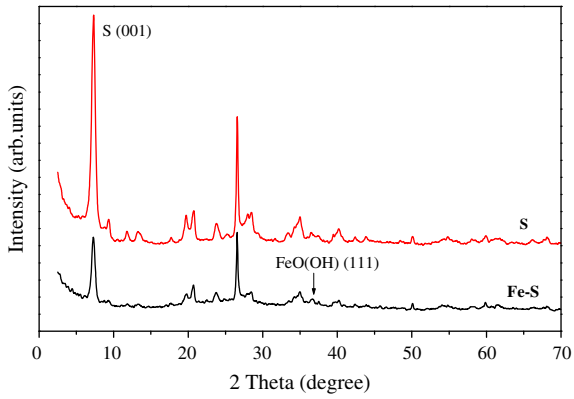

Fig. 4. XRD patterns of the S, the Fe–S and the Fe–S-673 composites.

respectively. The expansion in the basal spacing of the sepiolite attributes to the intercalation of iron oxide hydroxide, which is consistent with the results of the SEM analysis. The appearance of the diffraction peak at $2\theta = 33.0^{\circ}$, which is assigned to (222) reflection of Fe_2O_3 (JCPDS, file No. 32-0469), further confirms the existence of the iron oxide hydroxide in the Fe–S composites. Nitrogen adsorption/desorption isotherms of the Fe–S composites (Fig. 5) were measured, which revealed important structural characters of the as-prepared samples. The shape of the isotherm is type IV isotherm according to the IUPAC classification [35]. At high relative pressure between 0.4 and 1.0, the presence of a type H3 hysteresis loop would indicate some degree of mesoporosity. The mesoporous structure which combines lots of Fe_2O_3 particles may result from stacking defects inherent in the clay itself. The pore size distribution (inset in Fig. 5, calculated by BJH method) also shows a mesopore size distribution. The specific surface area and pore volume of the Fe–S were 217.68 m^2/g and 3.8743 cm^3/g, respectively, with 19 and 215% increment compared with the original sepiolite (183.56 m^2/g, 1.2297 cm^3/g). The improvement can be attributed to the mixture of pillared and partially delaminated clay structures.

3.3. Adsorption studies

3.3.1. Effect of pH

The UV–visible spectra of the MET aqueous solutions (10 mg/L) with different pH value are shown in Fig. 6. The absorbance of MET at 320 nm decreased and shifted to a shorter wavelength when the pH values decreased below the natural pH value of the MET aqueous solution (pH 7.0). The absorbance of the MET is almost constant when the pH value was higher than 7.0.

The UV–visible spectra of the MET aqueous solution over the Fe–S composites adsorption with pH values above 7.0 are shown in Fig. 7. The absorbance of the MET increased with the increase in pH values (pH > 7.0) when the absorbance was higher than that of the original MET (10 mg/L). The UV–visible spectra of the deionized water over the Fe–S composites adsorption with pH > 7.0 are also shown Fig. 7 (inset). The results indicate that MET cannot adsorb on the Fe–S composites effectively when the pH values are higher than 7.0. Therefore, the following discussion about the adsorption will be discussed under natural pH condition of the MET solution.

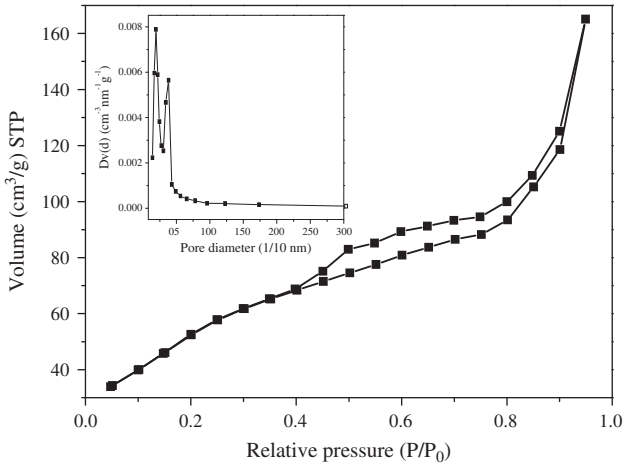

Fig. 5. N_2 adsorption/desorption isotherm and pore size distribution (inset) of the Fe–S.

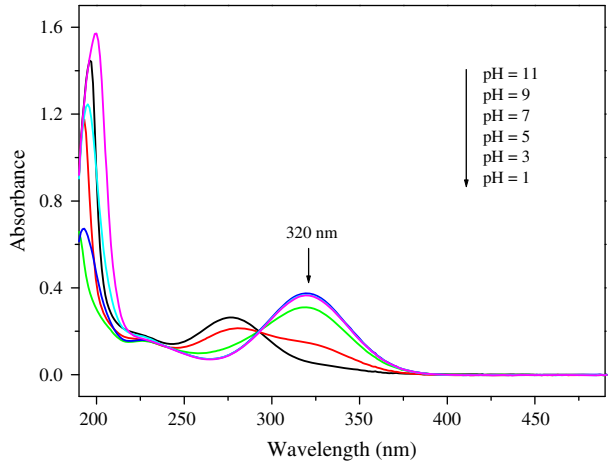

Fig. 6. The UV–visible spectral changes of MET aqueous solution (10 mg/L) with different pH values.

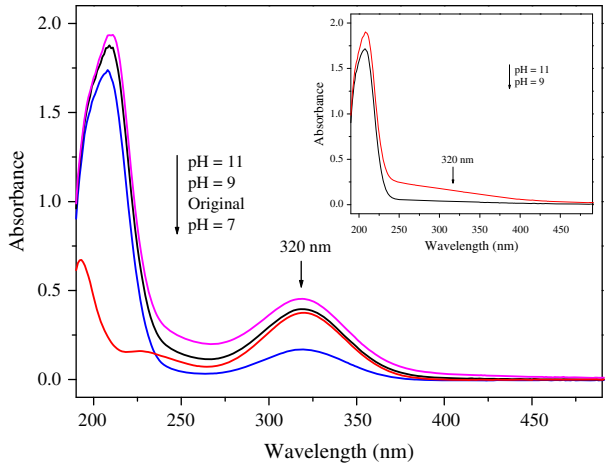

Fig. 7. The UV–visible spectral changes of MET aqueous solution over the Fe–S composites adsorption with different pH values. Inset: The UV–visible spectral changes of deionized water over the Fe–S composites adsorption with different pH values ([MET] = 10 mg/L, amount of Fe–S 0.2 g, at 303 K).

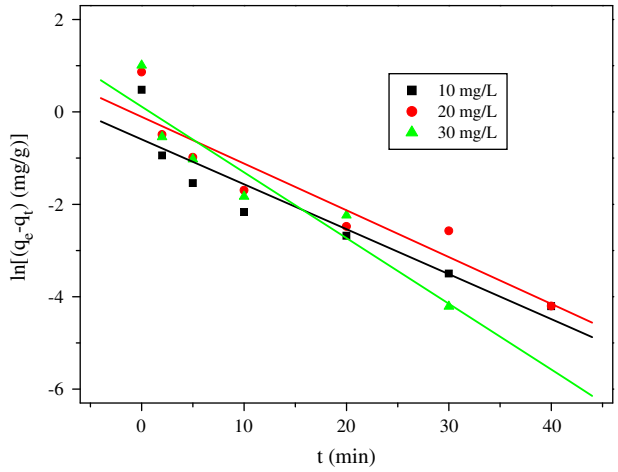

Fig. 9. Test of pseudo-first-order kinetic model for the adsorption of MET with different concentrations by Fe–S composites (amount of Fe–S 0.2 g, pH 7.0, at 303 K).

3.3.2. *Adsorption kinetics*

The effect of contact time on the adsorption of MET at different concentrations by Fe–S composites is shown in Fig. 8. The amounts of MET adsorbed on the Fe–S composites (q_t, mg/g) increased rapidly in 2 min. It is also observed that the amounts increased continuously, but the rates became slow with the increase in contact time and finally reached equilibrium after 10 min. This indicates that the MET adsorption on the Fe–S composites is a fast process, and nearly 90% of the adsorption takes place within 5 min.

Several kinetic models are available to describe the adsorption behavior of MET on Fe–S composites thus revealing the underpinning mechanism. In the present study, the adsorption data were analyzed using the pseudo-first-order [36,37] and pseudo-second-order [38,39] kinetic models.

The pseudo-first-order kinetic model can be expressed as Eq. (2),

$$dq_t/dt = k_1(q_e - q_t) \quad (2)$$

where q_e and q_t are the amount of MET adsorbed on the Fe–S composites at equilibrium and at time t,

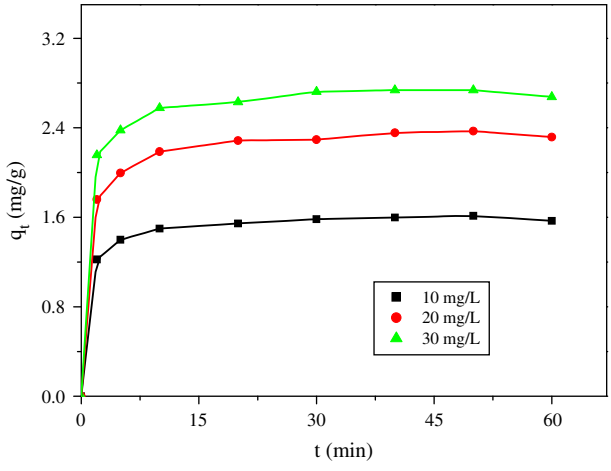

Fig. 8. Effect of contact time on the MET adsorption rate for different concentrations (amount of Fe–S 0.2 g, pH 7.0, at 303 K).

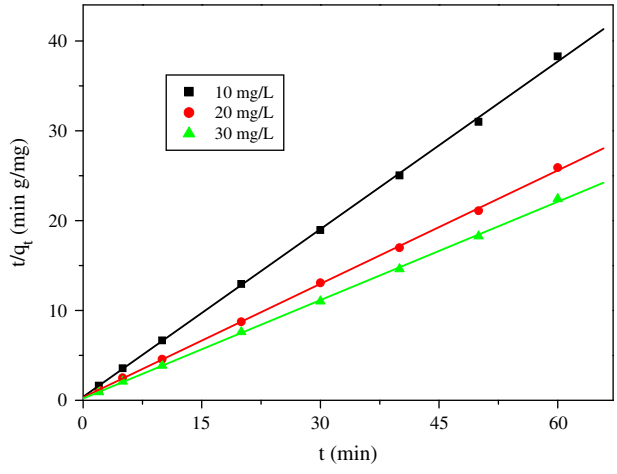

Fig. 10. Test of pseudo-second-order kinetic model for the adsorption of MET with different concentrations by Fe–S composites (amount of Fe–S 0.2 g, pH 7.0, at 303 K).

respectively (mg/g), and k_1 is the rate constant (1/min). Integrating and applying the boundary condition ($t = 0$ and $q_t = 0$, $t = t$ and $q_e = q_t$), Eq. (2) becomes Eq. (3),

$$\ln (q_e - q_t) = \ln q_e - k_1 t. \quad (3)$$

The pseudo-second-order kinetics model was also cited as Eq. (4),

$$dq_t/dt = k_2(q_e - q_t)^2 \quad (4)$$

where k_2 is the rate constant of pseudo-second-order adsorption (g/mg min). Integrating and applying the boundary condition ($t = 0$ and $q_t = 0$, $t = t$ and $q_e = q_t$), Eq. (4) takes the linear form as Eq. (5),

$$t/q_t = 1/k_2 q_e^2 + t/q_e \quad (5)$$

The linear plots ln ($q_e - q_t$) vs. t and t/q_t vs. t for the MET with different concentrations onto the Fe–S composites are shown in Figs. 9 and 10, respectively. The rate constant k, the calculated adsorption capacity $q_{e,cal}$, and the correlation coefficient R^2 for the pseudo-first-order kinetic model and the pseudo-second-order kinetic model are listed in Tables 1 and 2, respectively. It was found that the correlation coefficient for the pseudo-second-order kinetic model ($R^2 > 0.999$) was higher than that of the pseudo-first-order kinetic model ($R^2 > 0.877$). The $q_{e,cal}$ in the case of pseudo-second-order model fitted well with the experimental adsorption capacity $q_{e,exp}$ and a clear difference of $q_{e,cal}$ and $q_{e,exp}$ was observed in the case of pseudo-first-order model, which indicates that the adsorption data are better to be represented by pseudo-second-order kinetic model and the adsorption process is an irreversible chemisorption [38].

3.3.3. Adsorption isotherms

The effects of initial MET concentration on the adsorption are shown in Fig. 11. The equilibrium concentration of MET increased from 1.02 to 3.04 mg/g whereas the adsorption percentage decreased from 61.5 to 27.6% with the increase in the initial MET concentration from 5 to 50 mg/L. The results indicate that the initial MET concentration acts as a driving force to overcome mass transfer resistance for the MET transport between the aqueous solution and the surface of Fe–S composites. Meanwhile, MET in aqueous solution could not interact with the active binding sites of Fe–S composites due to the saturation of the sites at higher concentrations [40].

The Langmuir [41] and Freundlich [42] isotherm models were applied to the experimental data.

Table 1
Kinetic parameters of pseudo-first-order for the adsorption of MET with different concentrations by Fe–S composites (amount of Fe–S 0.3 g, at 303 K, pH 7.0)

		Pseudo-first-order		
C_0 (mg/L)	$q_{e,exp}$ (mg/g)	$q_{e,cal}$ (mg/g)	K_1 (1/min)	R^2
10	1.613	0.552	0.097	0.8771
20	2.370	0.900	0.101	0.8830
30	2.737	1.122	0.142	0.8937

Table 2
Kinetic parameters of pseudo-second-order for the adsorption of MET with different concentrations by Fe–S composites (amount of Fe–S 0.3 g, at 303 K, pH 7.0)

		Pseudo-second-order		
C_0 (mg/L)	$q_{e,exp}$ (mg/g)	$q_{e,cal}$ (mg/g)	K_2 (g/(mg min))	R^2
10	1.613	1.607	1.003	0.9995
20	2.370	2.375	0.537	0.9996
30	2.737	2.738	0.672	0.9995

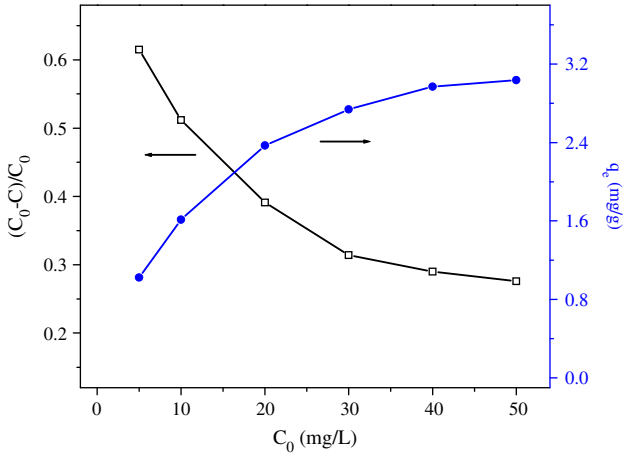

Fig. 11. Effect of initial MET concentration on the MET uptake and the adsorption capacity of the Fe–S composites (amount of Fe–S 0.2 g, pH 7.0, at 303 K).

The Langmuir isotherm model, which is valid for monolayer sorption onto a surface with a finite number of identical sites, may be expressed in the form as Eq. (6),

$$d\theta_t/dt = k_{ads}C_tN(1-\theta_t) - k_dN\theta_t \quad (6)$$

where N is the maximum number of adsorption sites occupied by MET and θ_t is the dimensionless surface coverage ratio ($\theta_t = q_t/q_m$). When the adsorption process reaches equilibrium, Eq. (6) yields Eq. (7),

$$C_e/q_e = 1/K_Lq_m + C_e/q_m \quad (7)$$

where $K_L = k_{ads}/k_d$ is the Langmuir constant including the affinity of binding sites (L/mg), q_m is the maximum adsorption capacity (mg/g), and q_e is the amount of MET adsorbed at equilibrium state (mg/g). q_e represents a practical limitation when the surface is fully covered with MET.

The Freundlich isotherm model is an empirical equation based on the adsorption on a heterogeneous surface, and is applicable to a multi-layer adsorption whose isotherm lacks a plateau. The relationship between the amount of MET adsorbed at equilibrium state (q_e, mg/g) and the equilibrium concentration of MET (C_e, mg/L) in the aqueous solution is,

$$q_e = K_FC_e^{1/n}. \quad (8)$$

Rearrange Eq. (8) and yield Eq. (9),

$$\ln q_e = \ln K_F + (1/n)\ln C_e \quad (9)$$

where K_F and n are Freundlich constants related to adsorption capacity and adsorption intensity, respectively, which depict whether the nature of adsorption is favorable or unfavorable. High K_F indicates a high adsorption capacity and high n ($n > 1$) indicates the good adsorption intensity over the entire range of the studied concentrations.

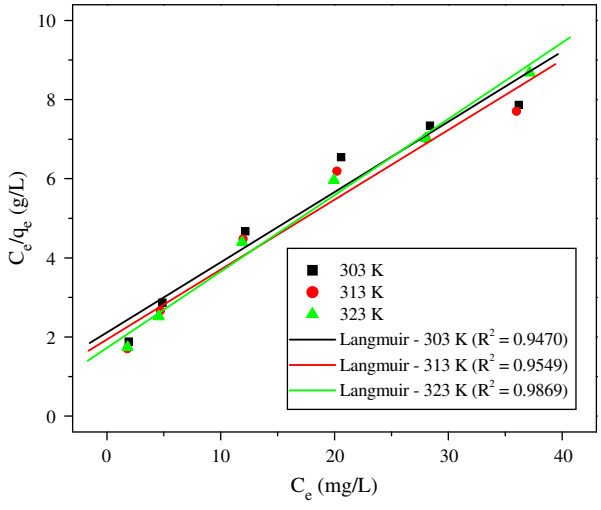

Fig. 12. Langmuir adsorption isotherms for the adsorption of the MET onto Fe–S composites at different temperatures (amount of Fe–S 0.2 g, pH 7.0).

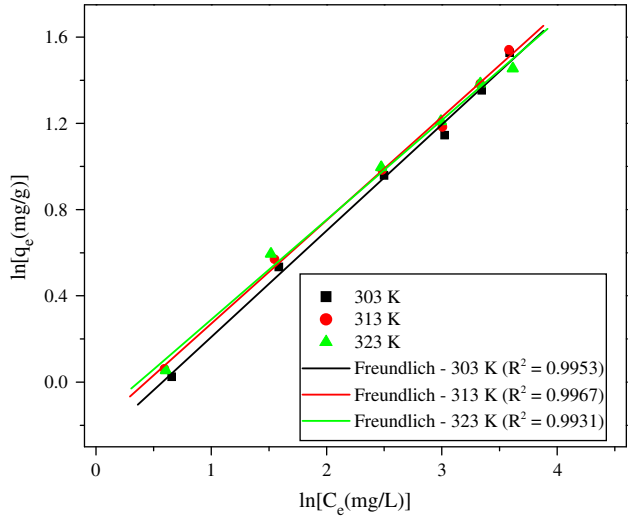

Fig. 13. Freundlich adsorption isotherms for the adsorption of the MET onto Fe–S composites at different temperatures (amount of Fe–S 0.2 g, pH 7.0).

Table 3
Parameters of Langmuir and Freundlich adsorption isotherm models for the MET on the Fe–S composites (amount of Fe–S 0.3 g, pH 7.0)

	Langmuir			Freundlich		
T (K)	q_m (mg/g)	K_L (L/mg)	R^2	K_F	n	R^2
303	5.618	0.084	0.9470	0.753	2.028	0.9953
313	5.650	0.091	0.9549	0.811	2.088	0.9967
323	5.181	0.112	0.9869	0.842	2.164	0.9931

Linear plots of C_e/q_e vs. C_e, ln q_e vs. ln C_e are shown in Figs. 12 and 13, respectively. The constant of q_m, K_L, K_F, and n are given in Table 3. The results show that the Freundlich model fits well with the experimental data. All n values are higher than 2.0, which indicate that the MET in aqueous solution can adsorb on the Fe–S composites. The value of K_F increases with the increase in temperature and the highest K_F value of 0.842 is obtained at a temperature of 323 K. The relatively lower value of K_F indicates that the adsorption capacity of the Fe–S composite for MET in aqueous solutions is low.

4. Conclusions

The sepiolite and modified sepiolite, by different methods, were applied in the removal of MET from aqueous solutions. The Fe–S composites show higher adsorption capacity (36.5%) than that of the original sepiolite and other modified sepiolites in this study. SEM and XRD analyses indicate that the iron oxide hydroxide exists in the Fe–S composites. The specific surface area and pore volume of the Fe–S increases from 183.56 to 217.68 m^2/g and 1.2297 to 3.8743 cm^3/g, respectively, compared with the original sepiolite. The MET adsorption on the Fe–S composites is a fast process. The pseudo-second-order rate model and the Freundlich adsorption isotherm model fits well with the experimental data.

Acknowledgments

This work was supported by the Natural Science Basic Research Plan in Shaanxi Province of China (2013JM7024).

References

[1] T.A. Larsen, J. Lienert, A. Joss, H. Siegrist, How to avoid pharmaceuticals in the aquatic environment, J. Biotechnol. 113 (2004) 295–304.
[2] C. Zwiener, F.H. Frimmel, Oxidative treatment of pharmaceuticals in water, Water Res. 34 (2000) 1881–1885.
[3] F. Gagné, C. Blaise, C. André, Occurrence of pharmaceutical products in a municipal effluent and toxicity to rainbow trout (*Oncorhynchus mykiss*) hepatocytes, Ecotoxicol. Environ. Saf. 64 (2006) 329–336.
[4] M. Carballa, F. Omil, J.M. Lema, M. Llompart, C. García-Jares, I. Rodríguez, M. Gómez, T. Ternes, Behavior of pharmaceuticals, cosmetics and hormones in a sewage treatment plant, Water Res. 38 (2004) 2918–2926.
[5] M.B. Johnson, M. Mehrvar, Aqueous metronidazole degradation by UV/H_2O_2 process in single- and multi-lamp tubular photoreactors: Kinetics and reactor design, Ind. Eng. Chem. Res. 47 (2008) 6525–6537.
[6] M.D. Hernando, M. Mezcua, A.R. Fernandezalba, D. Barcelo, Environmental risk assessment of pharmaceutical residues in wastewater effluents, surface waters and sediments, Talanta 69 (2006) 334–342.
[7] M. Klavarioti, D. Mantzavinos, D. Kassinos, Removal of residual pharmaceuticals from aqueous systems by advanced oxidation processes, Environ. Int. 35 (2009) 402–417.
[8] W. Gernjak, M.I. Maldonado, S. Malato, J. Cáceres, T. Krutzler, A. Glaser, R. Bauer, Pilot-plant treatment of olive mill wastewater (OMW) by solar TiO_2 photocatalysis and solar photo-Fenton, Solar Energ. 77 (2004) 567–572.
[9] H.R. Buser, T. Poiger, M.D. Müller, Occurrence and fate of the pharmaceutical drug diclofenac in surface waters: Rapid photodegradation in a lake, Environ. Sci. Technol. 32 (1998) 3449–3456.
[10] C. Zwiener, F.H. Frimmel, Short-term tests with a pilot sewage plant and biofilm reactors for the biological degradation of the pharmaceutical compounds clofibric acid, ibuprofen, and diclofenac, Sci. Total Environ. 309 (2003) 201–211.
[11] J.T. Yu, E.J. Bouwer, M. Coelhan, Occurrence and biodegradability studies of selected pharmaceuticals and personal care products in sewage effluent, Agric. Water Manage. 86 (2006) 72–80.
[12] K. Kümmerer, A. Al-Ahmad, V. Mersch-Sundermann, Biodegradability of some antibiotics, elimination of the genotoxicity and affection of wastewater bacteria in a simple test, Chemosphere 40 (2000) 701–710.
[13] S.A. Snyder, S. Adham, A.M. Redding, F.S. Cannon, J. DeCarolis, J. Oppenheimer, E.C. Wert, Y. Yoon, Role of membranes and activated carbon in the removal of endocrine disruptors and pharmaceuticals, Desalination 202 (2007) 156–181.

[14] S.D. Kim, J. Cho, I.S. Kim, B.J. Vanderford, S.A. Snyder, Occurrence and removal of pharmaceuticals and endocrine disruptors in South Korean surface, drinking, and waste waters, Water Res. 41 (2007) 1013–1021.
[15] K. Fent, A.A. Weston, D. Caminada, Ecotoxicology of human pharmaceuticals, Aquat. Toxicol. 76 (2006) 122–159.
[16] A. Özcan, E.M. Öncü, A.S. Özcan, Kinetics, isotherm and thermodynamic studies of adsorption of acid blue 193 from aqueous solutions onto natural sepiolite, Colloids Surf., A 277 (2006) 90–97.
[17] A. Tabak, E. Eren, B. Afsin, B. Caglar, Determination of adsorptive properties of a Turkish sepiolite for removal of reactive blue 15 anionic dye from aqueous solutions, J. Hazard. Mater. 161 (2009) 1087–1094.
[18] G. Rytwo, S. Nir, L. Margulies, B. Casal, J. Merino, E. Ruiz-Hitzky, J.M. Serratosa, Adsorption of monovalent organic cations on sepiolite: Experimental results and model calculations, Clays Clay Miner. 46 (1998) 340–348.
[19] M. Shirvani, H. Shariatmadari, M. Kalbasi, F. Nourbakhsh, B. Najafi, Sorption of cadmium on palygorskite, sepiolite and calcite: Equilibria and organic ligand affected kinetics, Colloids Surf., A 287 (2006) 182–190.
[20] M. Alkan, G. Tekin, H. Namli, FTIR and zeta potential measurements of sepiolite treated with some organosilanes, Micropor. Mesopor. Mater. 84 (2005) 75–83.
[21] Y.R. Park, Synthesis, characterisation and application of organic surfactants modified clays for water purification[D], Ph.D. Thesis, Brisbane, 2013.
[22] Y. Turhan, P. Turan, M. Doğan, M. Alkan, H. Namli, Ö. Demirbaş, Characterization and adsorption properties of chemically modified sepiolite, Ind. Eng. Chem. Res. 47 (2008) 1883–1895.
[23] M. Akçay, FT-IR spectroscopic investigation of the adsorption pyridine on the raw sepiolite and Fe-pillared sepiolite from Anatolia, J. Mol. Struct. 694 (2004) 21–26.
[24] E. González-Pradas, M. Villafranca-Sánchez, M. Socías-Viciana, M. Fernández-Pérez, Preliminary studies in removing atrazine, isoproturon and imidacloprid from water by natural sepiolite, J. Chem. Technol. Biotechnol. 74 (1999) 417–422.
[25] H. Chen, A.Q. Wang, Adsorption characteristics of Cu (II) from aqueous solution onto poly(acrylamide)/attapulgite composite, J. Hazard. Mater. 165 (2009) 223–231.
[26] J.E.D. Davies, N. Jabeen, The adsorption of herbicides and pesticides on clay minerals and soils. Part 1. Isoproturon, J. Inclusion Phenom. Macrocyclic Chem. 43 (2002) 329–336.
[27] E.A. Ferreiro, S.G. de Bussetti, Thermodynamic parameters of adsorption of 1,10-phenanthroline and 2,2´-bipyridyl on hematite, kaolinite and montmorillonites, Colloids Surf., A 301 (2007) 117–128.
[28] H. Cheng, J. Yang, R.L. Frost, Thermogravimetric analysis-mass spectrometry (TG-MS) of selected Chinese palygorskites—Implications for structural water, Thermochim. Acta 512 (2011) 202–207.
[29] H. Düskünkorur, Biopolyester synthesis by enzymatic catalysis and development of nanohybrid systems[D], Ph.D. Thesis, Strasbourg, 2012.
[30] J.X. Li, J. Hu, G.D. Sheng, G.X. Zhao, Q. Huang, Effect of pH, ionic strength, foreign ions and temperature on the adsorption of Cu(II) from aqueous solution to GMZ bentonite, Colloids Surf., A 349 (2009) 195–201.
[31] W.-F. Lee, Y.-C. Chen, Effect of intercalated reactive mica on water absorbency for poly(sodium acrylate) composite superabsorbents, Eur. Polym. J. 41 (2005) 1605–1612.
[32] H. Shemer, Y.K. Kunukcu, K.G. Linden, Degradation of the pharmaceutical MET via UV fenton and photofenton processes, Chemosphere 63 (2006) 269–276.
[33] R.F. Dantas, O. Rossiter, A.K.R. Teixeira, A.S.M. Simões, V.L.D. da Silva, Direct UV photolysis of propranolol and metronidazole in aqueous solution, Chem. Eng. J. 158 (2010) 143–147.
[34] P.N. Bartlett, E. Ghoneim, G. Elhefnawy, I. Elhallag, Voltammetry and determination of metronidazole at a carbon fiber microdisk electrode, Talanta 66 (2005) 869–874.
[35] A. Lam, A. Rivera, G. Rodrídguez-Fuentes, Theoretical study of metronidazole adsorption on clinoptilolite, Micropor. Mesopor. Mater. 49 (2001) 157–162.
[36] E. Manova, P. Aranda, M.A. Angeles Martín-Luengo, S. Letaĭef, E. Ruiz-Hitzky, New titania-clay nanostructured porous materials, Micropor. Mesopor. Mater. 131 (2010) 252–260.
[37] G.W. Brindley, G. Brown, Crystal Structures of Clay Minerals and their X-ray Identification, Mineralogical Society, London, 1984.
[38] S. Lagergren, Zur theorie der sogenannten adsorption gelöster stoffe (Theory of adsorption substances from solution), Kungliga Svenska Vetenskapsakademiens, Handlingar 24 (1898) 1–39.
[39] Y.S. Ho, G. McKay, Pseudo-second order model for sorption processes, Process Biochem. 34 (1999) 451–465.
[40] V.C. Srivastava, M.M. Swamy, I.D. Mall, B. Prasad, I.M. Mishra, Adsorptive removal of phenol by bagasse fly ash and activated carbon: Equilibrium, kinetics and thermodynamics, Colloids Surf., A 272 (2006) 89–104.
[41] I. Langmuir, The constitution and fundamental properties of solids and liquids. Part I. Solids, J. Am. Chem. Soc. 38 (1916) 2221–2295.
[42] H. Freundlich, Über die adsorption in lösungen (Adsorption in solution), Z. Phys. Chem. 57 (1906) 385–470.